THE EVALUATION OF CRACK RESISTANCE AND CRACK VELOCITY FROM CONTROLLED FRACTURE EXPERIMENTS OF CERAMIC BEND SPECIMENS

F. W. Kleinlein and H. Hübner*

INTRODUCTION

The crack resistance R of a material when loaded in mode I and in a given environment (e.g. humid air) depends on the crack velocity $\dot{a}$, the crack length a, and, in some cases, on the way how the crack length had been achieved. In a controlled fracture experiment stable crack propagation occurs and an equilibrium is maintained between the crack resistance and the applied energy release rate G_I:

$$R = G_I. \tag{1}$$

Under these experimental conditions R can be determined from the well known equation

$$G_I = (P^2/2B)\ dC/da \tag{2}$$

where C is the compliance of the specimen. The dependence of R on Δa mainly has been determined on metallic materials [1]. In the case of glass and ceramics, the measurement of the R ($\dot{a}$) and $K_I(\dot{a})$ relationship has been reported in the literature [2,3] using DCB and DT specimens respectively. These sample types show some drawbacks: large size of the specimen, complicated machining, and difficulties in uniaxial loading at least of DCB specimens. As to our knowledge, no attempts have been made so far to determine the crack resistance and the $\dot{a}$,R-relationship of ceramic materials on SENB type specimens.

In this paper a method is presented to evaluate both the crack resistance and the crack velocity from controlled fracture tests on notched bend specimens loaded in four-point bending. The method is applied to experiments performed on polycrystalline Al_2O_3 and on glass, and the results are compared with crack velocity data published in the literature.

To obtain stable crack propagation the geometry of the SENB specimens was optimized [4] according to the work of J. Nakayama [5] and D. P. Clausing [6]. During fracture propagation both the load-displacement and the load-time diagram was recorded. For any desired point of the load-displacement record the crack length a can be determined from the specimen compliance using the K calibrations Y(a/W) given by W. F. Brown and J. E. Srawley [7] and by W. K. Wilson [8] respectively.

*Institute of Materials Science, University Erlangen-Nürnberg, West Germany.

EVALUATION METHOD

The crack resistance in a given point i of the load-displacement record is computed from equations (1) and (2). The load P_i immediately can be taken from the diagram, whereas the term dC/da is determined from the well known equation

$$dC/da = 9(l_o-e)^2(1-\nu^2)Y^2(a/W)/(2BW^3E). \quad (3)$$

In equation (3), l_o and e are the lower and the upper span length respectively. The elastic constants E and ν must be determined experimentally. The crack length, a, is difficult to be measured continuously by optical microscopy, quite apart from the fact that effects of crack front bowing and pinning are not taken care of, by only measuring the crack depth on the side faces of opaque materials. For this reason, a is determined from the instantaneous specimen compliance using equation (3) which yields after integration:

$$C(a) = C_o + \frac{9(l_o-e)^2(1-\nu^2)}{2BW^2E} \int_o^a Y^2(a'/W)d(a'/W) \quad (4)$$

Here C_o is the compliance of the unnotched specimen which is given by

$$C_o = (l_o-e)^2(l_o+2e)/(4BW^3E) \quad (5)$$

where the effect of shear stresses is neglected [9]. Since the K calibration Y as a function of a is known even for a/W values near unity [8], a can be determined for a given experimental value of C by a numerical solution of equation (4).

To determine the specimen compliance C_i in a given point i of the load-displacement record the displacement must be corrected for the elastic deformations of the machine parts to yield the true specimen deflection. This is due to the fact that in our experimental set-up which is shown in Figure 1 only the displacement between the loading ram C and the support plate E can be recorded. This displacement s consists of the deflection of the sample s_C and of the elastic deformations s_A of all parts of the bending apparatus lying between the loading ram and the support plate: $s = s_C+s_A$. As described in section 3, $s_A(P)$ easily can be measured for a four-point bending set-up. Thus, for any given value of P_i the specimen deflection $s_{C,i}$ is obtained by subtracting $s_A(P_i)$ from the total displacement s_i:

$$s_{C,i} = s_i - s_A(P_i) \quad (6)$$

By that way the true load-deflection curve can be constructed point-by-point. It is characterized by a steeper increase and a smaller decrease of the load compared with the original load-displacement record. Figure 2 shows an example for this procedure. The corrected curve 3 is obtained by subtracting the apparatus curve 1 from the measured record 2.

The second step of the evaluation method consists in determining compliance values from the corrected curve. From the very linear elastic increase of the corrected load-deflection curve a straight line is obtained by a least squares best fit method which defines the origin of the plot as indicated in Figure 2. The inverse slope of the straight line gives the compliance value which pertains to the initial crack length a_o. The compliance C_i in any point i and with the crack length a_i is obtained from the slope of the straight line which is drawn from $(P_i, s_{C,i})$ to the origin. By inserting C_i into equation (4), solving for a_i, and inserting into equations (3), (2) and (1), for a given i a data point (R_i, a_i) can be computed. By applying this procedure to a series of data points of the controlled fracture record the $R(\Delta a)$ curve is obtained quasi-continuously.

In the last stage of the evaluation process a time value t_i is attributed to each data point i from the load-time record. The mean velocity of the crack between the points i and i+1 is given by

$$\dot{a}_i = (a_{i+1}-a_i)/(t_{i+1}-t_i), \quad (7)$$

and the mean crack resistance pertaining to $\dot{a}_i$ is

$$\bar{R}_i = (R_{i+1}+R_i)/2. \quad (8)$$

Equations (7) and (8) define one data point of the $\dot{a}$,R-relationship.

EXPERIMENTAL PROCEDURE

The bending device shown in Figure 1 is operated in an Instron 114 testing machine. The displacement is measured with an inductive gauge (sensitivity about 2 mV/µm). The compliance curve of the bending apparatus can easily be recorded by adjusting the lower rollers exactly beneath the upper rollers. Loading this set-up yields a record of load vs. all additional elastic deformations of the bending device as shown in Figure 2 (curve 1). Even the elastic depressions of the specimen at the loading points are included.

The materials used in this investigation were a soda lime glass, pure Al_2O_3 (grain size 20 µm), and an Al_2O_3-2wt.-per cent Cr_2O_3 solid solution (grain size 6 µm). The samples were bars of the size 4x5x50 mm. The opposite side faces were ground parallel. The width W varied within ± 2 µm along the length of the sample. Test pieces of Al_2O_3 were centre through notched with a diamond cutting blade of 0.1 mm thickness resulting in a notch width of about 0.15 mm. It has been shown by R. L. Bertolotti [10] that this notch root radius represents a sufficient sharp pre-crack for polycrystalline alumina. In the case of glass samples, however, only uncontrolled failure could be achieved using this type of notch. Therefore, a triangular notch according to [11] was cut into the specimens which causes a large stress concentration at the tip of the triangle. Using this type of notch, fully stable crack propagation could be obtained. The evaluation of these experiments, however, was limited to that region of specimen width where a centre through crack was reached ($a/W \approx 0.7$).

Once crack propagation had started two different types of machine operation were carried out. In type 1 the testing machine was driven with a constant cross-head speed throughout the test. In type 2 the cross-head was stopped to get nearly fixed-grip conditions (with the exception of some small deflection increase due to the elastic extension of the machine parts within the gauge length). Type 2 operation is characterized by an enlarged range of stable cracking, i.e. smaller notch depths may be used.

Most of the experiments were carried out in air of natural humidity which roughly amounted to 50 to 80 per cent. One glass experiment was performed in silicon oil (0 per cent humidity).

RESULTS

In Figure 3 some crack resistance curves are plotted against the relative crack length a/W. As was to be expected, the crack resistance of glass is independent of the crack length. The small decrease at very large a/W values is due to the large decrease of the crack velocity at the end of the experiment.

The crack resistance of Al_2O_3, however, shows an increasing trend for all crack length values. Three regions can be observed. Starting with the initial crack length, a_o, R increases rapidly and then turns into region 2 of constant slope which extends to a/W~0.9. In region 3 the crack resistance increases strongly again. Both the magnitude of R and the slope of region 2 depend on the grain size of the material, the coarse grained material having higher values.

The mean value of R averaged over the crack length range from a_o to W

$$\bar{R} = \int_{a_o}^{W} R da/(W-a_o) \qquad (9)$$

turns out to be twice the specific work of fracture γ_F. According to [5], γ_F is the work supplied by the machine, i.e. the area under the load-deflection curve, divided by the area of the two created fracture surfaces. In terms of the γ_F definition, R may be regarded as a "differential work of fracture". The results of the experiments shown in Figure 3 are, in J/m^2, $\bar{R}$ = 61.4 and $2\gamma_F$ = 62.4 for the fine grained Al_2O_3, and $\bar{R}$ = 83.6 and $2\gamma_F$ = 84.3 for the coarse grained material respectively.

Figure 4 shows $\dot{a}$,R-results on soda lime glass compared with data from the literature [2,12]. The data points ▼ mark an experiment with controlled humidity (0 per cent) and correspond to the crack resistance curve of glass shown in Figure 3.

DISCUSSION

The crack velocity data evaluated from our SENB experiments are in reasonably good agreement with results on DCB specimens [2,12] although a complete quantitative comparison is not possible because of the lack of controlled humidity. The result of constant crack resistance of glass as a function of the crack length up to very large a-values confirms the

validity of Wilson's calibration function [8] which already has been verified experimentally up to a/W = 0.91 in our laboratory [13].

The crack resistance curves of Al_2O_3 show the somewhat astonishing fact of considerably increasing R with increasing crack length. This means that Al_2O_3 becomes a tougher material once a natural crack has developed. An interpretation of this behaviour based on secondary crack formation and on fracture surface interference is given in [14]. The measurement of R curves possibly could explain the discrepancy between work of fracture values γ_F of Al_2O_3 [11,15] and values of the specific surface energy of fracture initiation γ_I as determined from K_{Ic} [16,17] which turns out to be about one third of γ_F.

As to the validity and accuracy of our evaluation method, two experimental studies have been performed concerning both the determination of the crack length from the specimen compliance and the correction procedure to obtain the true sample deflection. Crack length values computed from compliance have been compared with optical crack length measurements on notched bars [14]. A reasonably good agreement could be observed. By application of the correction procedure to loading experiments of unnotched bars the static Young's modulus was found to agree with values determined dynamically within 2 per cent [13].

ACKNOWLDGEMENT

This work was sponsored by the Deutsche Forschungsgemeinschaft.

REFERENCES

1. Fracture Toughness Evaluation by R Curve Methods, ASTM STP 527 1973.
2. WIEDERHORN, S. M., J. Amer. Ceram. Soc. 50, 1967, 407.
3. EVANS, A. G., J. Mater. Sci. 7, 1972, 1137.
4. KLEINLEIN, F. W. and HÜBNER, H., to be published.
5. NAKAYAMA, J., J. Amer. Ceram. Soc. 48, 1965, 583.
6. CLAUSING, D. P., Int. J. Fracture Mech. 5, 1969, 211.
7. BROWN, W. F. and SRAWLEY, J. E., Plane Strain Fracture Toughness Testing of High-Strength Metallic Materials, ASTM STP 410, 1966.
8. WILSON, W. K., Engng. Fract. Mech. 2, 1970, 169.
9. LUBAHN, J. D., Proc. ASTM 59, 1959, 885.
10. BERTOLOTTI, R. L., J. Amer. Ceram. Soc. 56, 1973, 107.
11. TATTERSALL, H. G. and TAPPIN, G., J. Mater. Sci 1, 1966, 296.
12. RICHTER, H., Scientific Report 9/74, Inst. f. Festkörpermechanik, Freiburg 1974.
13. HÜBNER, H. and SCHUHBAUER, H., submitted to Int. J. Fracture
14. HÜBNER, H. and JILLEK, W., submitted to J. Mater. Sci.
15. DAVIDGE, R. W. and TAPPIN, G., J. Mater. Sci. 3, 1968, 165.
16. SWANSON, G. D., J. Amer. Ceram. Soc. 55, 1972, 48.
17. SIMPSON, L. A., J. Amer. Ceram. Soc. 56, 1973, 7.

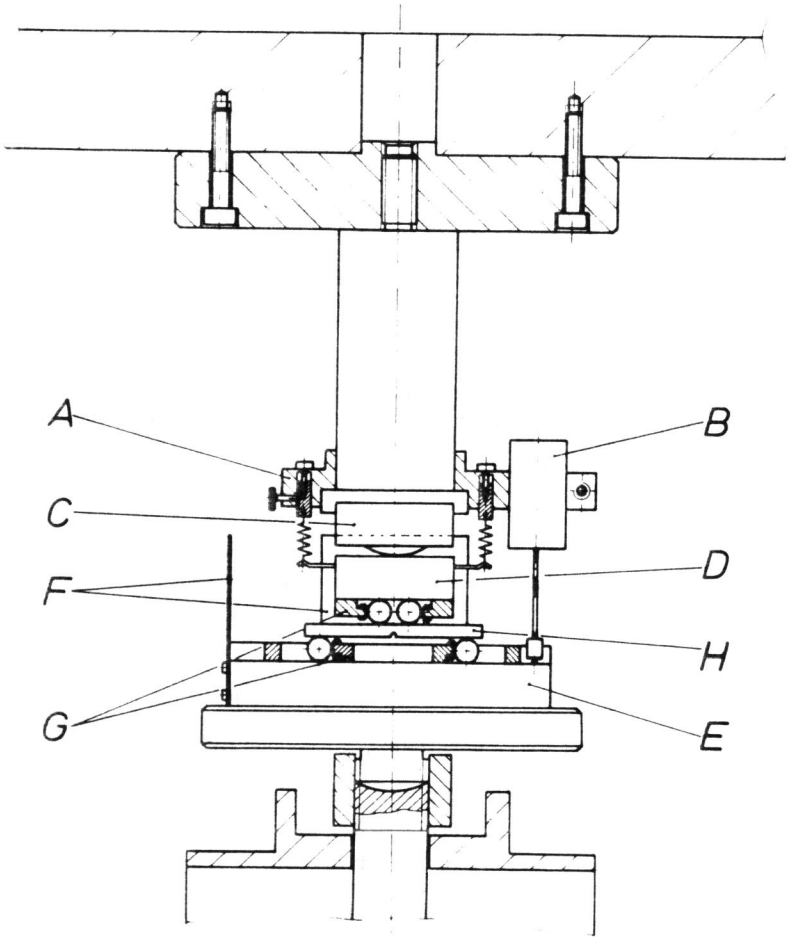

Figure 1 Four-Point Bending Set-up

A: Adjustment Facility
B: Displacement Gauge
C: Loading Ram
D: Loading Plate and Upper Rollers
E: Support Plate
F: Adjustment Mirrors
G: Electromagnetic Fixing of Rollers
H: Bend Specimen

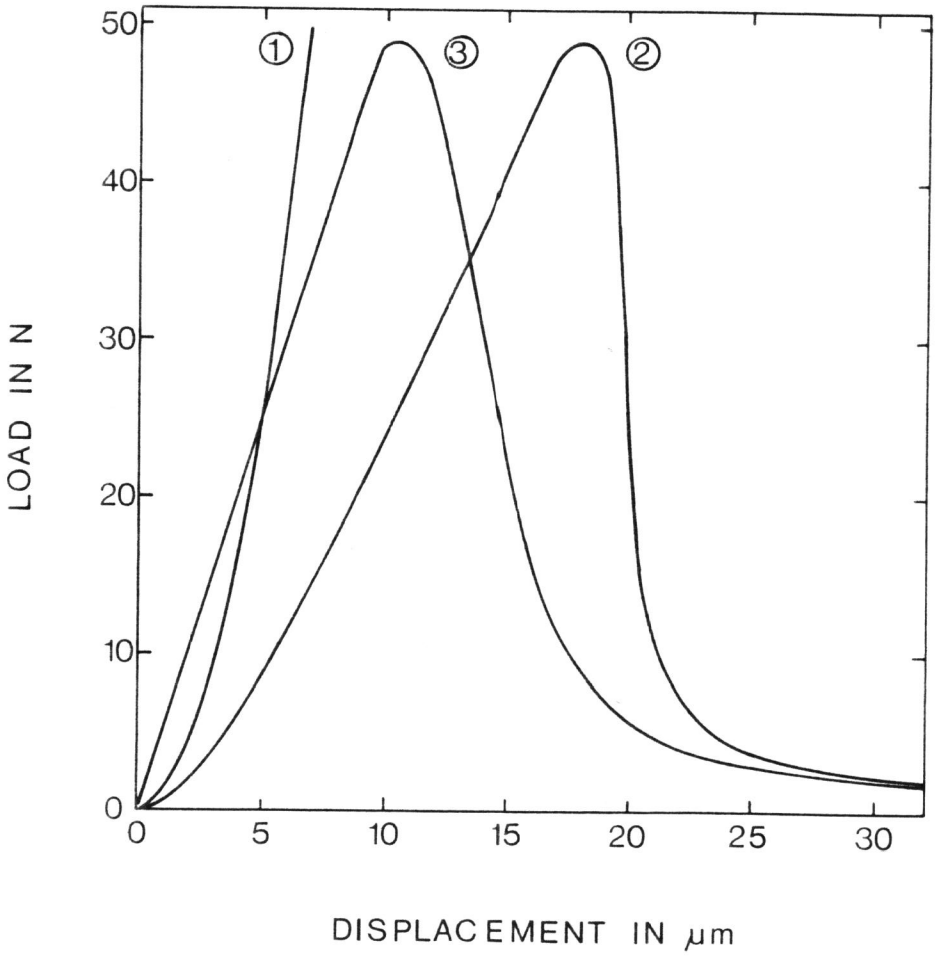

Figure 2 Load-Displacement Curves

Curve 1: Bending device only.
Curve 2: Bending device plus bend specimen (1 and 2 as-recorded).
Curve 3: True load-deflection diagram of the specimen obtained from curve 2 by subtracting the apparatus deformations of curve 1.

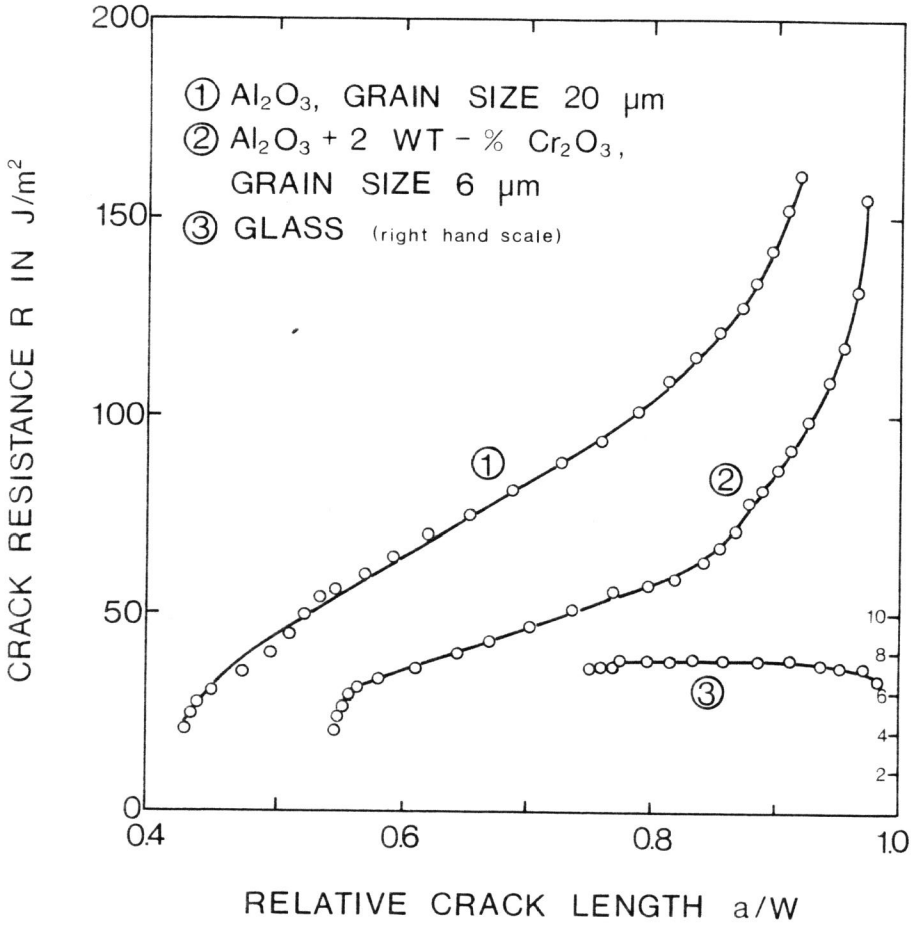

Figure 3 Crack resistance of Al_2O_3 and of an Al_2O_3-Cr_2O_3 solid solution compared to glass.

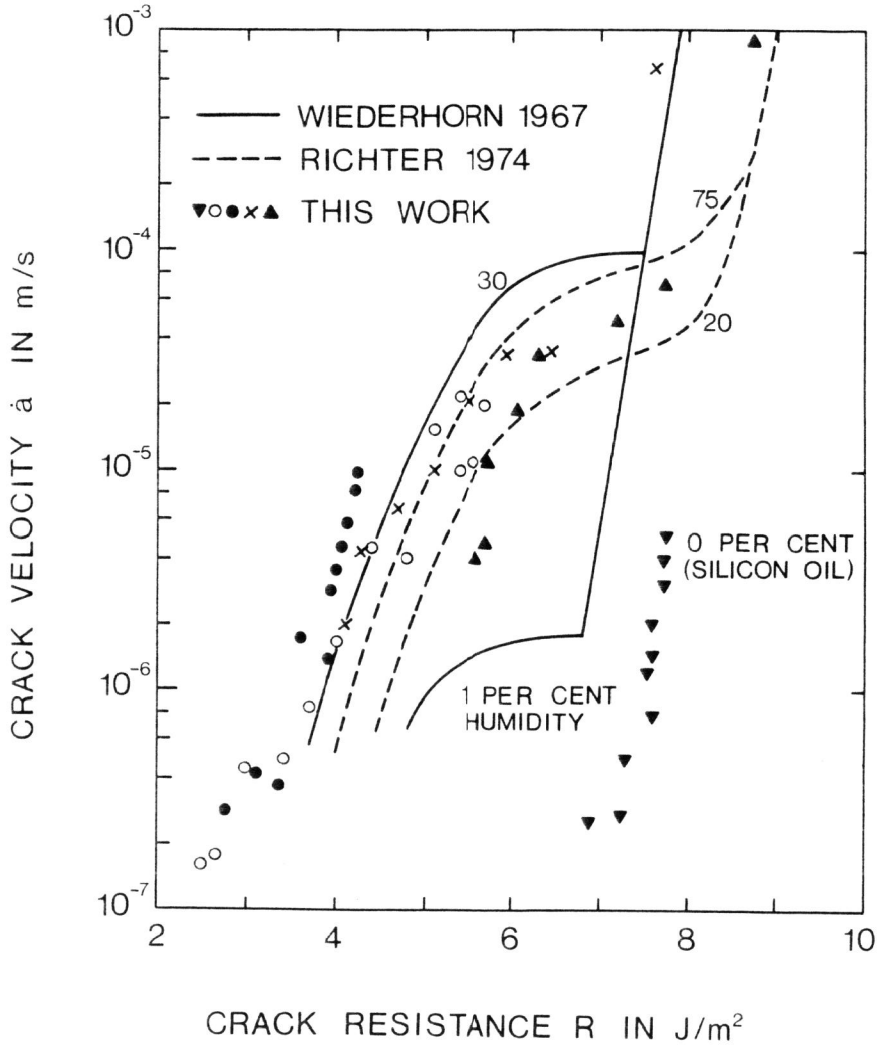

Figure 4 Crack Velocity Measurements on Glass. Experimental data on bend specimens are compared with results on DCB specimens reported in the literature.